RSC Advances

ROYAL SOCIETY
OF CHEMISTRY

www.rsc.org/advances

1   **Preparation of naphthyl functionalized magnetic nanoparticles for**

2   **extraction of polycyclic aromatic hydrocarbons from river waters**

3

4   Ying Cai[#], Zhi-Hong Yan[#], Ni-Ya Wang, Qing-Yun Cai [*], Shou-Zhuo Yao

5

6   State Key Laboratory of Chemo/Biosensing & Chemometrics, College of Chemistry

7   & Chemical Engineering, Hunan University, Changsha 410082, China

8   **ABSTRACT**

9   A novel core/shell structured magnetic sorbent, naphthyl functionalized magnetic

10   nanoparticles ($Fe_3O_4@SiO_2@Nap$), were prepared and successfully applied for the

11   magnetic solid-phase extraction (MSPE) of polycyclic aromatic hydrocarbons (PAHs)

12   from river water samples. The analytes were finally determined by high performance

13   liquid chromatography coupled with fluorescence detection (HPLC-FLD). Seven

14   kinds of PAHs were selected as the model analytes, including fluorene (Flu),

15   fluoranthene (Fla), anthracene (Ant), pyrene (Pyr), benz[a]anthracene (BaA),

16   benzo[b]fluoranthene (BbF) and benzo[k]fluoranthene (BkF). Transmission electron

17   microscopy (TEM), vibrating sample magnetometer (VSM), fourier transform

18   infrared spectrometry (FTIR) and X-ray photoelectron spectroscopy (XPS) were used

19   to characterize the sorbent. The main influencing parameters including sorbent

20   amount, desorption solvent, sample volume and extraction time were optimized to

*Corresponding author. Tel.: +86-73188821848. E-mail: qycai0001@hnu.edu.cn,
qycai0002@gmail.com.
[#] These authors contributed equally to this study and share first authorship.

21 achieve the highest recovery rate. Under the optimal conditions, only 40 mg of

22 $Fe_3O_4@SiO_2@Nap$ sorbent was used to extract PAHs. The linear ranges of all the

23 seven PAHs were 0.5-100 ng L^{-1} with the limits of detection (S/N = 3) ranging from

24 0.04 to 0.12 ng L^{-1}. The repeatability was investigated by evaluating the intra- and

25 inter-day precisions with relative standard deviations (RSDs) lower than 4.3%. Finally,

26 the proposed method was successfully applied for the determination of PAHs in river

27 water samples with the recoveries in the range of 89.6-106.8%.

28 **Keywords:** Magnetic solid-phase extraction; Polycyclic aromatic hydrocarbons;

29 Environmental analysis; π-π interaction.

30 **1. Introduction**

31　　Polycyclic aromatic hydrocarbons (PAHs) comprise a large group of

32 compounds with two or more fused benzene rings. They are widespread

33 environmental contaminants that result from incomplete combustion of organic

34 materials during natural or anthropogenic processes. PAHs are toxic substances

35 which are resistant to degradation. Numerous epidemiological studies indicate that

36 exposed people have increased risks of cancer.[1] PAHs are therefore considered as

37 priority pollutants by both the US Environmental Protection Agency (EPA) and the

38 European Environmental Agency.[2,3] Consequently, there are increasing interests in

39 the detection of PAHs in environmental water sources for the protection of health

40 and the environment. PAHs are hydrophobic in nature with low water solubility,

41 being less soluble in water and less volatile with increasing molecular weight.[4] To

42 determine trace PAHs in aquatic environments by instrumental analysis, sample

43   pre-concentration technique is usually required. Solid-phase extraction (SPE) is one

44   of the most commonly used techniques for the preconcentration of PAHs.[5] SPE has

45   been widely exploited due to its strong separation capacity, high enrichment factor,

46   minimal sample and solvent consumption, low cost and easy automation.[6]

47   Nowadays, a new mode of SPE, magnetic solid-phase extraction (MSPE)

48   technology,[7] has received increasing attention. Based on the use of magnetic

49   nanoparticles, it has high extraction efficiency and rapid extraction kinetics.

50   Magnetic nanoparticles (MNPs) are provided with many merits such as good

51   stability, easy synthesis, high surface area, facile separation by magnetic forces, as

52   well as low toxicity and low cost, and therefore have been widely applied in

53   environmental and material science.[8] The magnetic nanoparticles are always directly

54   dispersed in the sample solutions to quickly extract analytes since they can be readily

55   recovered by a magnet. Compared with traditional SPE, MSPE sorbents combine

56   numerous advantages such as large surface area, unique magnetic property,

57   convenient functional modification, high separation efficiency, high reusability and

58   environmental friendliness.[9] MSPE shows great potential applications in

59   preconcentration and separation.[10-14] Typically, the magnetic nanoparticles were

60   composed of a magnetic core (Fe_3O_4) and a functionalized shell which can

61   selectively adsorb targets.[15]   Various functionized magnetic nanoparticles were

62   synthesized as sorbents to extract trace PAHs from various environmental matrices,

63   including carbon coated Fe_3O_4 nanoparticles (Fe_3O_4/C),[16,17] alkyl (C_{10}-C_{18})

64   carboxylates,[18] n-octadecylphosphonic acid modified mesoporous magnetic

65   nanoparticles (OPA/MMNPs), [14] C_{18}-functionalizedmagnetic nanoparticles,[19-22]

66   diphenyl functionalization of Fe_3O_4 magnetic nanoparticles (Fe_3O_4-diphenyl),[15]

67   Fe_3O_4-doped poly(styrene-divinylbenzene-co-4-vinylbenzenesulfonic acid sodium

68   salt) nanoparticles (Fe_3O_4-MPNP),[3] phosphatidylcholine bilayer coated magnetic

69   nanoparticles (Fe_3O_4/PC),[23] cholesterol-functionalized magnetic nanoparticles

70   (Fe_3O_4@SiO_2@Chol),[24] polydopamine coated Fe_3O_4 nanoparticles (Fe_3O_4/PDA),[25]

71   magnetic microsphere-confined graphene (Fe_3O_4@SiO_2-G),[26] metal-organic

72   framework MIL-101,[27] triphenylamine-functionalized magnetic

73   microparticles(Fe_3O_4/SiO_2/TPA),[28] ionic liquid coated magnetic nanoparticles

74   (IL-MNPs)[29] and magnetic nanoparticles-nylon 6 composite.[30]

75   In this work, we developed a new kind of MNPs termed as naphthyl

76   functionalized magnetic silica nanoparticles (Fe_3O_4@SiO_2@Nap) to extract PAHs

77   from river water samples. To our knowledge, this is the first report on the introduction

78   of naphthyl to functionalized magnetic nanoparticles for the extraction of PAHs. The

79   condensed cyclic structure and hydrophobic property of naphthyl is expected to make

80   it a good functional material to interact with PAHs through the π-π conjugative effect,

81   which would increase the selectivity of the sorbent to PAHs. The proposed MNPs

82   were applied successfully for the extraction of PAHs in three kinds of river water

83   samples. Finally, according to the USA Environmental Protection Agency Method

84   610,[31] PAH priority pollutants must be determined using HPLC in combination with

85   ultraviolet absorption or fluorescence detectors. We used high performance liquid

86   chromatography coupled with fluorescence detection (HPLC-FLD) to determine

87 PAHs.

88 **2. Experimental**

89 2.1. Chemicals

90   Ferric chloride hexahydrate ($FeCl_3 \cdot 6H_2O$, 99%), ferrous sulfate heptahydrate

91 ($FeSO_4 \cdot 7H_2O$, 99%), ammonia (26%), hydrazine hydrate (99%), isopropanol (99%),

92 triethylamine (99%), toluene (99%) and naphthoyl chloride (99%) were purchased

93 from Sinopharm Chemical Reagent Co. Ltd. (China). Methanol and acetonitrile of

94 HPLC grade (99%) were bought from Merck (Darmstadt, Germany).

95 Tetraethoxysilane (TEOS, 99%) and 3-isocyanatopropyltriethoxysilane (ICPTES,

96 99%) were obtained from Adamas Reagent Ltd. (Switzerland). Other reagents

97 including n-hexane, acetone, methanol, isopropanol and ethanol were of analytical

98 grade. Ultrapure water was prepared using a Milli-Q system water purification

99 system (Millipore Inc., USA). It was degassed using an ultrasonic bath for 5 min

100 prior to use.

101   Certified reference standards of fluorene (Flu, 99%), fluoranthene (Fla, 99%),

102 anthracene (Ant, 99%), pyrene (Pyr, 99%), benzo[a]anthracene (BaA, 99%),

103 benzo[b]fluoranthene (BbF, 99%) and   benzo[k]fluoranthene (BkF, 99%) were

104 purchased from Acros Organics (NJ, USA).

105   Stock PAH solutions were prepared in HPLC grade methanol containing Flu, Ant,

106 Pyr (1 mg mL^{-1}), Fla (1 mg mL^{-1}), BaA (0.05 mg mL^{-1}), BbF and BkF (0.5 mg mL^{-1}),

107 and kept at 4 ºC in darkness. Working solutions of PAHs composed of Flu, Ant, Pyr,

108 BbF, BkF (100 ng mL^{-1}), Fla (200 ng mL^{-1}) and BaA (50 ng mL^{-1}) was prepared by

109   diluting the stock solutions with methanol.

110   2.2. Apparatus

111   The size and morphological characterization of the particles were observed by

112   transmission electron microscopy (TEM, JEM-2100F, JEOL Co., Tokyo, Japan).

113   Fourier transform infrared spectra (FTIR) were recorded on Vertex 70 (Bruker Optics,

114   Germany). X-ray photoelectron spectroscopy (XPS) was tested on a Thermo

115   ESCALAB 250Xi X-ray photoelectron spectrometer (Thermo Scientific, USA).

116   Samples were dried at 80 ºC in a vacuum oven for 12 h, and mixed with KBr to

117   fabricate a KBr pellet for FTIR analysis. PAHs were extracted from water samples

118   with assistance of an ultrasonic instrument KQ-600KDE. The magnetic property was

119   analyzed using a vibrating sample magnetometer (VSM, Model 7410，Lake Shore

120   Cryotronics, Inc., Westerville, Ohio, USA).

121   Chromatographic separations and analysis of PAHs were carried out on an

122   Agilent 1260 Series HPLC system (Agilent, USA) including a G1311C quatpump, a

123   G1322A degasser, a G1329B auto-sampler, a G1316A column oven and a G1321A

124   fluorescence detector (FLD).Agilent Chem Station was used to control the system and

125   the process of the chromatographic data. The chromatographic separation of PAHs

126   was performed using an Ultimate XB-C_{18} column (5 μm particle diameter, 3.0 mm i.d.

127   × 250 mm length, Ultimate, Welch Materials, Inc.) with a column oven temperature

128   maintained at 30 ºC. The mobile phase consisted of methanol-water (v/v 85/15) at a

129   flow rate of 1.0 mL min^{-1}. The excitation and emission wavelength programs used for

130   the fluorescence detection were listed in Table S1.

131 2.3. Preparation of $Fe_3O_4@SiO_2@Nap$ MNPs

132 2.3.1. Preparation of Fe_3O_4 MNPs

133   The Fe_3O_4 magnetic nanoparticles (MNPs) were prepared by chemical

134 co-precipitation. Briefly, $FeCl_3 \cdot 6H_2O$（4.0 g）was dissolved in deionized water (30

135 mL) in a three-necked round bottom flask, followed by addition of hydrazine hydrate

136 (2 mL) and $FeSO_4 \cdot 7H_2O$ (10.90 g) to prepare a stock solution. Afterwards, ammonia

137 (35 mL 26.5% w/w) was added into the stock solution under vigorous stirring,

138 followed by dropwise addition of ammonia until the solution pH reached 9. Then it

139 was stirred at room temperature for 30 min, aged at 80 ºC for 60 min, and then

140 cooled to room temperature. The product was magnetically collected, and washed

141 with water, finally vacuum-dried at 60 ºC for 12 h.

142 2.3.2. Encapsulation of the MNPs with silica $(Fe_3O_4@SiO_2)$

143   Nanoparticles (1 g) were dispersed in a mixture of 2-propanol (100 mL) and

144 ultrapure water (8 mL), sonicated for 15 min, followed by addition of ammonia (10

145 mL) and TEOS (8 mL) sequentially. The mixture was then stirred for 12 h at 45 ºC.

146 The magnetic nanoparticles were collected by a magnet and washed with water and

147 ethanol respectively and vacuum-dried at 60 ºC for 12 h. In this step, the

148 ferromagnetic nanoparticles were encapsulated with a mesoporous silica shell.

149 2.3.3. Preparation of naphthyl coated MNPs $(Fe_3O_4@SiO_2@Nap)$

150   The preparation scheme of $Fe_3O_4@SiO_2@$ Nap is depicted in Fig. 1. For this

151 purpose, 40 mL of anhydrous toluene, 3.0 g of naphthoyl chloride, 1 mL of

152 triethylamine and 2.5 mL of ICPTES were added to a 150 mL three-neck

153   round-bottom flask under argon. The mixture was refluxed for 24 h at 80 ºC under

154   magnetic stirring, and cooled slowly to room temperature. Two grams of the dried

155   silica gel-modified magnetic nanoparticles were added to the solution. The mixture

156   was then refluxed for 12 h at 110 ºC under mechanical stirring in argon atmosphere.

157   The as-prepared product was magnetically collected and washed by n-hexane, acetone

158   and ethanol successively. The resulting $Fe_3O_4@SiO_2@Nap$ was dried under vacuum

159   at 60 ºC for 12 h.
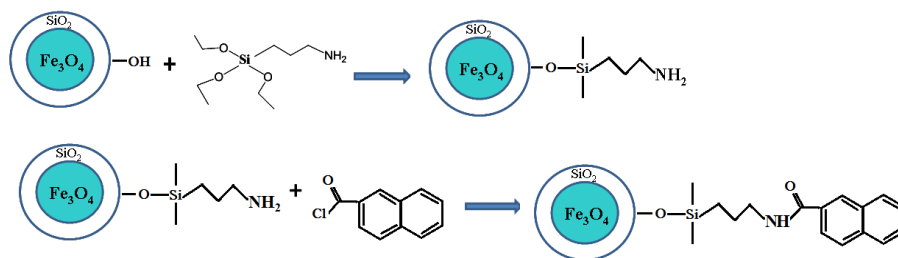
160

161   Fig.1. Preparation scheme of $Fe_3O_4@SiO_2@Nap$

162   2.4. Sample collection

163   River water samples were collected from different districts of Nanchang city in

164   September 2014. Yudai river water was collected from Yudai River (Nanchang,

165   Jiangxi, China), Qingshan Lake water was collected from Qingshan Lake (Nanchang,

166   Jiangxi, China), and the Ganjiang River water was collected from the Ganjiang River

167   (Nanchang, Jiangxi, China). All samples were collected at 10 cm depth below the

168   water surface, filtered through 0.45µm cellulose membranes to remove suspended

169   particles, and stored in an amber glass bottle at 4 ºC. The filtered water samples were

170   analyzed within 24 h.

171   2.5. MSPE procedure

172   Forty mg of $Fe_3O_4@SiO_2@Nap$ was placed in a 250 mL vial and firstly activated

173   with methanol, then dispersed into 150 mL of water sample spiked with the proper

174   amounts of PAHs. After being sonicated for 30 s to form a homogeneous dispersion

175   solution, the magnetic nanoparticles were isolated rapidly from the solution by

176   applying an external magnetic field for 12 min. After decanting the supernatant

177   solution, the captured PAHs were desorbed by 1.0 mL of acetonitrile. The desorption

178   solution was collected and filtered through a 0.22 μm polytetrafluoroethylene (PTFE)

179   membrane syringe filter, 20 μL of the filtrate was injected into HPLC for analysis.

180   **3. Results and discussion**

181   3.1 Characterization of $Fe_3O_4@SiO_2@Nap$ MNPs

182   The prepared MNPs were characterized with TEM, VSM,   FTIR and XPS.

183   The TEM image of Fig.S1a shows that the Fe_3O_4 nanoparticles exhibit spherical

184   morphologies with an average diameter of 20 nm. The TEM image of Fig.S1b shows

185   that the obtained $Fe_3O_4@SiO_2$ MNPs at an average diameter of 120 nm are with a

186   dark magnetite core and a uniform gray silica shell which provides abundant silanol

187   groups for further chemical modification. The $Fe_3O_4@SiO_2@Nap$ (Fig. S1c) are

188   larger than $Fe_3O_4@SiO_2$ in size, due to the modification of naphthyl.

189   The magnetic properties of the prepared MNPs were investigated with a

190   vibrating sample magnetometer (VSM). Fig.2a shows the magnetization curves of

191   Fe_3O_4, $Fe_3O_4@SiO_2$ and $Fe_3O_4@SiO_2@Nap$ at 300 K, giving the magnetic saturation

192   values of 71.6, 30.73 and 27.56 emu/g, respectively. The coating results in decreases

193   in the magnetic saturation values of $Fe_3O_4@SiO_2$ and $Fe_3O_4@SiO_2@Nap$. It was

194 reported that a saturation magnetization of 16.3 emu g^{-1} is sufficient for a magnetic

195 separation with a magnet.[32] Thus, the Fe$_3$O$_4$@SiO$_2$@Nap sorbents loaded with

196 analytes can be readily separated from solution with magnet due to their

197 superparamagnetism and large saturation magnetization.

198   FTIR analysis was employed to confirm the surface groups of the as- synthesized

199 MNPs. FTIR spectra depicted in Fig.2b are acquired for bare Fe$_3$O$_4$, Fe$_3$O$_4$@SiO$_2$ and

200 Fe$_3$O$_4$@SiO$_2$@Nap MNPs between 4000 and 400 cm^{-1}. Two characteristic absorption

201 peaks at 3400 and 590 cm^{-1} are assigned to the stretching vibrations of hydroxyl

202 groups of the hydrogen-bonded surface water molecules and the Fe-O-Fe transverse

203 vibration of Fe$_3$O$_4$ NPs, respectively. Coating of SiO$_2$ onto Fe$_3$O$_4$ NPs was

204 demonstrated by the appearance of characteristic peaks at 1090 and 466 cm^{-1}

205 (spectrum b and c), corresponding to the Si-O-Si stretching vibration and Si-O

206 symmetric stretching vibration, respectively. The weak bands at 2850 and 2929 cm^{-1}

207 are assigned to the stretching vibrations of C-H bonds. After modification with

208 naphthyl, there displays a prominent peak at 806 cm^{-1}, which is characteristic of –H

209 on naphthalene ring. In addition, a band at 1540 cm^{-1} corresponds to the bending

210 vibration of skeleton of aromatic ring appears. These results confirmed the success

211 surface modification of the magnetic nanoparticles.

212   To determine the chemical composition and to further affirm   the   modification

213 on the surface of Fe$_3$O$_4$@SiO$_2$@Nap MNPs, the X-ray photoelectron spectroscopy

214 analysis is employed. The C 1s, N 1s, O 1s and Si 2p deconvolution XPS spectra for

215 Fe$_3$O$_4$@SiO$_2$@Nap are analyzed by curve fitting. As seen in Fig.2c, the C 1s

216   deconvolution spectra exhibit four components of the carbon bond at 284.4 eV

217   (C=C/C-H), 284.6 eV (C-C/C-H), 285.4 eV (C-C aromatic) and 288.6 eV (C=O).

218   The N 1s deconvolution spectra exhibit the nitrogen bond at 399.5 eV (N-C) and

219   399.8 eV (N-H). The O 1s deconvolution spectra exhibit three components of the

220   oxygen bond at 532.4 eV (O=C) and 532.7 eV (-C=O/SiO_2), and Si 2p

221   deconvolution spectra also exhibit SiO_2 (103.1 and 103.7 eV). In addition, the atomic

222   ratio of the surface of Fe_3O_4@SiO_2@Nap is obtained from XPS data, and C/N/O/Si

223   ratio is 20.53/3.3/51.1/24.67. The ratio of O/Si is approximately 2:1, which conforms

224   to the construction of Fe_3O_4@SiO_2@Nap. But there may be some non-bonded SiO_2

225   on the surface of Fe_3O_4@SiO_2@Nap because of high ratio of Si/N. The number of

226   carbon atoms may be associated with alkyl carbon and carbon atoms on naphthalene

227   ring.

228   3.2. Optimization of extraction conditions

229   Several parameters that may affect the extraction efficiency were optimized，

230   such as the sorbent amount, types of desorption solvent，solution volume and

231   extraction time. The influence of all these parameters was evaluated in terms of

232   recovery rate. The optimization experiments were conducted using pure water spiked

233   with Flu, Ant, Pyr, BbF, BkF (10 ng L^{-1}), Fla (20 ng L^{-1}) and BaA (5 ng L^{-1}). Each

234   experiment was performed in triplicate.

235

236

237   (a)   (b)

238

239

240   (c)
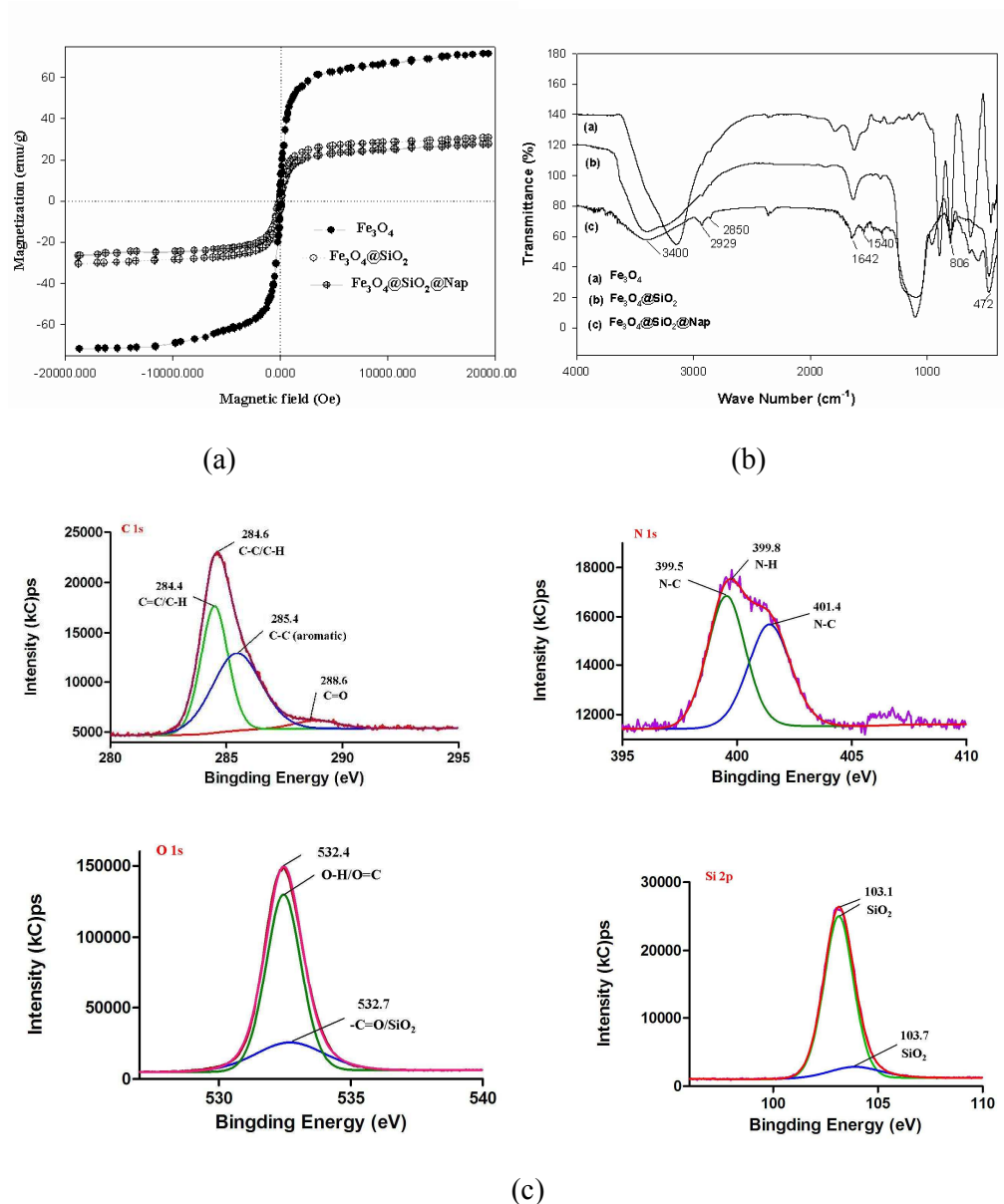
241 Fig.2. Magnetization curves of Fe_3O_4, $Fe_3O_4@SiO_2$ and $Fe_3O_4@SiO_2@Nap$ (a),

242   FTIR spectroscopy of Fe_3O_4, $Fe_3O_4@SiO_2$ and $Fe_3O_4@SiO_2@Nap$ (b),

243   Detail and deconvoluted XPS spectra of C 1s, N 1s, O 1s and Si 2p for

244        $Fe_3O_4@SiO_2@Nap$ (c).

245

246 3.2. Optimization of extraction conditions

247   Several parameters that may affect the extraction efficiency were optimized，

248 such as the sorbent amount, types of desorption solvent，solution volume and

249 extraction time. The influence of all these parameters was evaluated in terms of

250 recovery rate. The optimization experiments were conducted using pure water spiked

251 with Flu, Ant, Pyr, BbF, BkF (10 ng L^{-1}), Fla (20 ng L^{-1}) and BaA (5 ng L^{-1}). Each

252 experiment was performed in triplicate.

253 3.2.1. Effect of the sorbent amount

254 The sorbent amount is a key parameter affecting the extraction efficiency,

255 which was investigated with various amounts of $Fe_3O_4@SiO_2@Nap$ MNPs under the

256 conditions of 150 mL sample volume, 1.0 mL acetonitrile as desorption solvent, and

257 12 min extraction time. Figure 3a shows that the recovery rates of all the tested

258 PAHs increase continuously with the increase of the sorbent amount from 10 to 40

259 mg. Further increasing the sorbent amount over 40 mg results in no obvious change

260 in the recovery. These results indicate that 40 mg of sorbents are sufficient to extract

261 PAHs. Excess sorbent may retain analytes resulting in the decrease in recovery. So,

262 40 mg of sorbent was used for the following experiments. Apparently, the required

263 amount of $Fe_3O_4@SiO_2@Nap$ in this work is far less than the amount of traditional

264 SPE (C-18) sorbents.[33-35]

265 3.2.2. Effect of the desorption solvent

266 A complete desorption of analytes from the sorbent is highly related to the

267 organic solvent. Five types of solvents were selected as desorption solvent, including

268 acetonitrile, methanol, acetonitrile/isopropanol (v/v 1/1), acetone, and n-hexane.

269 While other conditions were as follows: amount of sorbent, 40 mg; sample volume:

270 150 mL; and extraction time, 12 min. In order to achieve the best recoveries,

271    $Fe_3O_4@SiO_2@Nap$ nanoparticle sorbents were sonicated for 30 s in desorption

272   solvents. As shown in Fig. 3b, acetonitrile yields the highest recovery for all of the

273   tested PAHs. Hence, acetonitrile was used as the desorption solvent throughout the

274   experiments.

275

(a)   (b)

276

(c)   (d)
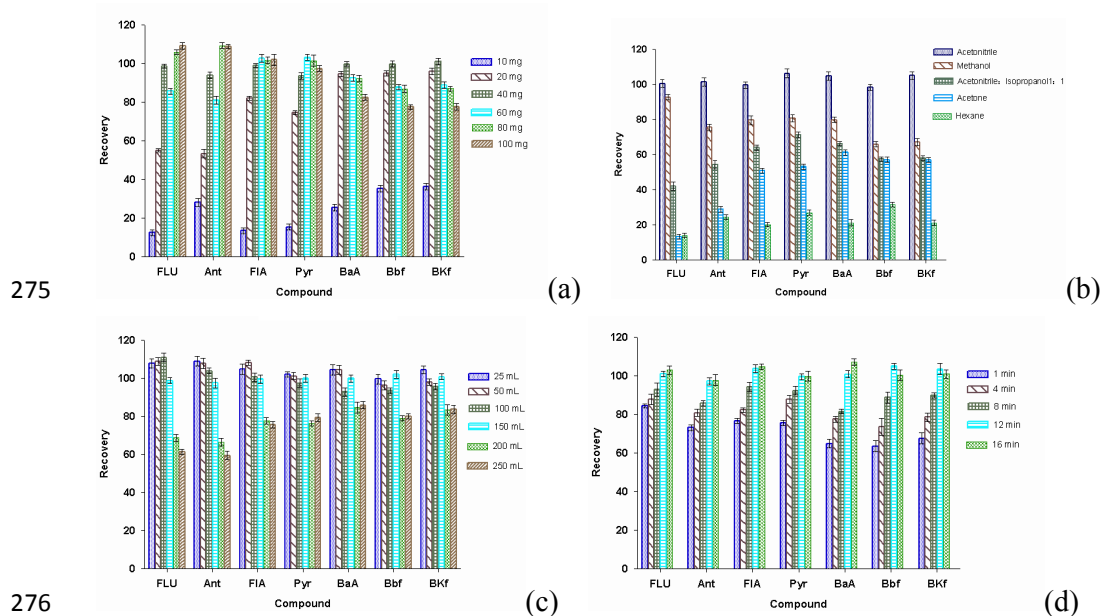
277   Fig.3. Effect of (a) amount of sorbent, (b) different desorption solvent, (c) the sample volume, (d)

278   extraction time on the extraction recoveries of PAHs.

279   3.2.3. Effect of sample volume

280   The sample volume from 10 to 250 mL was tested under conditions of 40 mg

281   amount of sorbent, 1.0 mL acetonitrile as desorption solvent, and 12 min extraction

282   time. As shown in Fig. 3c, the recovery rates of all the PAHs do not change

283   significantly with increasing the sample volume from 10 to 150 mL. Further

284   increasing the sample volume over 200 mL resulted in decreased in the recovery

285   rates. The sample volume was therefore selected as 150 mL. The enrichment

286   factors，defined as the ratio of the concentration of analytes in the final desorption

287   solvent (1 mL acetonitrile) to the initial concentration of the analyte in the sample

288   solution (150 mL), were determined to be 163, 141, 154, 139, 147, 145, and 149 for

289   Flu, Ant, Fla, BaA, Pyr, BbF and BkF, respectively.

290   3.2.4. Effect of the extraction time

291   The recovery is also dependent on the extraction time which was evaluated

292   within the range from 1 to 16 min under conditions of 40 mg sorbent, 150 mL sample

293   volume, and 1.0 mL acetonitrile as the desorption solvent. As can be seen in Fig.3d,

294   12 min was sufficient to achieve satisfactory extraction. Therefore, extraction time of

295   12 min was applied in the MSPE procedure.

296   Based on the above experimental results, the optimal conditions for MSPE of

297   PAHs were as below: 40 mg of $Fe_3O_4@SiO_2@Nap$ MNPs, 1.0 mL acetonitrile as

298   thedesorption solvent, 150 mL solution volume, and 12 min of the extraction time.

299

300   3.3 Investigation of the extraction mechanism

301   To prove that naphthyl played an important role on the extraction of PAHs, the

302   extraction capacities of naked Fe_3O_4, $Fe_3O_4@SiO_2$ and $Fe_3O_4@SiO_2@Nap$ were

303   compared under the same conditions. The results are shown in Fig. 4. It can be seen

304   that bare Fe_3O_4 has little enrichment ability towards PAHs, while $Fe_3O_4@SiO_2$ has

305   better extraction capacity but recoveries of PAHs were all below 40%.

306   $Fe_3O_4@SiO_2@Nap$ shows the best extraction performance towards 7 PAHs, which

307   are more hydrophobic. The condensed cyclic structure and hydrophobic property of

308   naphthyl is expected to make it a good sorbent to interact with PAHs through the π-π

309   conjugative effect and hydrophobic interaction, which would improve the enrichment

310 abilities of the sorbent to PAHs. The results show that naphthyl on the surface of

311 sorbent results in a significant improvement of extraction efficiency towards the

312 PAHs.
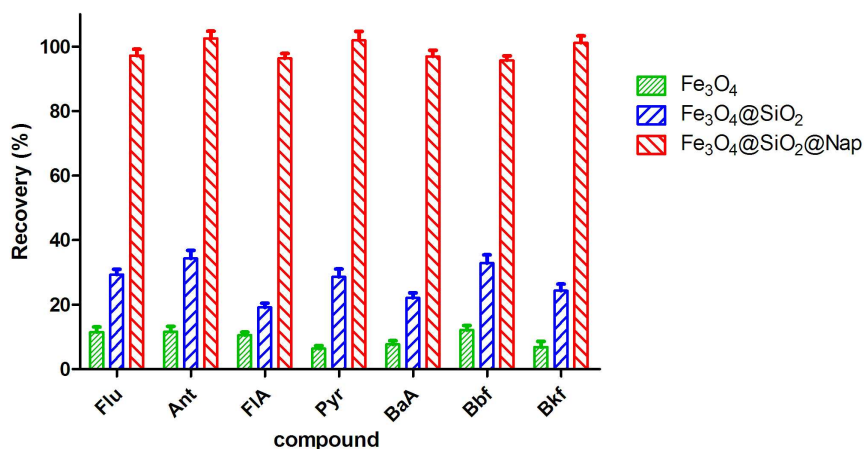
313

314   Fig.4 Comparison of different sorbents on the extraction efficiencies of PAHs.

315 3.4 Reusability of $Fe_3O_4@SiO_2@Nap$

316   In order to investigate the recycling of the nanoparticle sorbents, the used

317 $Fe_3O_4@SiO_2@Nap$ (40 mg) was regenerated by rinsing it with 1 mL of acetonitrile

318 twice to make sure that no PAHs was remianed in the sorbent. Then the regenerated

319 sorbent was applied in MSPE. The recoveries of PAHs are listed in Fig.S2. After 10

320 times of regeneration, there are no obvious changes in the recoveries of analytes with

321 the used $Fe_3O_4@SiO_2@Nap$ as sorbent, indicating that the $Fe_3O_4@SiO_2@Nap$

322 sorbents are stable and durable during MSPE procedure.

323 3.5. Analytical characteristics

324   Under the optimized conditions, a series of experiments with regard to the

325 linearity, limit of detection (LOD), and precision were performed to validate the

326 proposed method. In order to investigate the possible matrix effect on determination,

327   the linearity of the proposed method was estimated by analyzing different standard

328   solutions with various concentration of PAHs (0.5, 5, 10, 25, 50, 100 ng L^{-1}) in

329   Ganjiang river water sample. Six-point calibration curve was constructed by plotting

330   peak area vs PAH concentrations. Intra-day and inter-day precision were calculated in

331   terms of RSD% (five replicates) obtained with real water sample spiked with 5 ng L^{-1}

332   PAHs.

333   The achieved results of the validation procedure are listed in Table 1. The

334   calibration curves were linear in the range of 0.5-100 ng L^{-1} with coefficient of

335   determination ranging from 0.9983 to 0.9997. The limit of detection (LOD) and the

336   limit of quantification (LOQ) were calculated as the concentrations of the analytes at a

337   signal-to-noise ratio (S/N) of 3 and 10, respectively. Our results show that the LOD

338   and LOQ of the PAHs range from 0.04 to 0.12 ng L^{-1} and 0.15 to 0.40 ng L^{-1},

339   respectively. The relative standard deviations (RSDs) for the PAHs were below 4.3%,

340   illustrating a good repeatability. These results imply that the proposed method can be

341   applied to the analysis of real samples containing PAHs at trace level.

342   Table 1 Figures and merit of the MSPE method for the determination of PAHs in water

PAHs	Calib. Curve [a](n=3)	Linear range (ng L^{-1})	R^2	LOQ (ng L^{-1})	LOD (ng L^{-1})	RSD (n=5) (%)	
						Intra-day	Inter-day
Flu	y= 4100.62x + 276.88	0.5-100	0.9992	0.20	0.064	0.6	1.1
Ant	y = 8500.8x + 686.88	0.5-100	0.9983	0.15	0.044	0.7	2.0
FlA	y = 500.8959x + 73.842	0.5-100	0.9991	0.25	0.081	0.8	1.6
Pyr	y = 3900.216x + 206.45	0.5-100	0.9995	0.38	0.120	2.3	4.3
BaA	y = 4500.824x + 271.02	0.5-100	0.9997	0.40	0.095	1.1	2.0
BbF	y = 800.7977x + 86.625	0.5-100	0.9994	0.16	0.048	0.8	1.3
BKF	y = 6200.638x + 266.95	0.5-100	0.9993	0.26	0.085	1.2	3.0

343   [a] x is compound concentration (ng L^{-1}) and y is peak area.

17

344   3.6. Analysis of river water samples

345   Three kinds of river water sampled from Yudai River, Qingshan Lake and

346   Ganjiang River were analyzed under optimized conditions. Aliquots of 150 mL of

347   each sample were filtered through a 0.45 μm cellulose membrane, and then spiked

348   with the PAHs at three concentration levels (0.5, 5 and 10 ng L^{-1}). The spiked

349   samples were stored in dark overnight, and then analyzed by the proposed method

350   (n=3). Fig. 5 shows typical chromatograms of MPSE of river water samples and

351   river water samples spiked with PAHs. The results are listed in Table 2. Anthracene

352   and fluoranthene were found in both Yudai river water samples and Qingshan Lake

353   water samples. At the same time, anthracene and pyrene were found in Ganjiang

354   water samples. The relative recoveries of PAHs at three concentration levels are in

355   the range of 89.6-106.8%, with RSDs within 5.9%. These results imply that the

356   established method can be applied to the analysis of PAHs at trace level in real

357   samples.
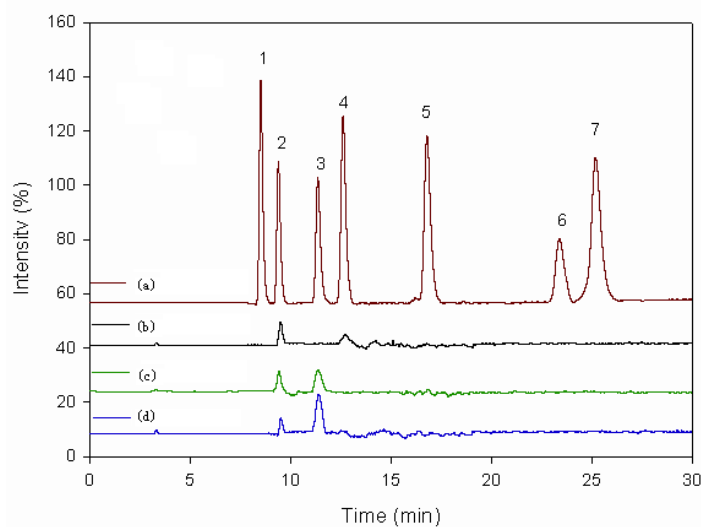
358

359   Fig.5. Magnetic solid-phase extraction HPLC-FLD chromatograms of river water samples. (a)

360   Qingshan Lake river water sample spiked with 5 ng L^{-1} of each analyte; (b) Ganjiang river water

361   sample; (c) Qingshan Lake river water sample and (d)Yudai river water sample. Peak assignment:

362   (1) Flu, (2) Ant, (3) Fla, (4) Pyr, (5) BaA, (6) BbF, (7) BkF.

363   3.7 Comparison of $Fe_3O_4@SiO_2@Nap$ with other sorbents

364   The extraction efficiencies of $Fe_3O_4@SiO_2@Nap$ to target PAHs were compared

365   with other magnetic materials including Fe_3O_4/C,[16-17] C_{10}-C_{18} carboxylates,[18]

366   OPA/MMNPs,[14] Fe_3O_4-C_{18},[19-21] Fe_3O_4-MPNP,[3] Fe_3O_4/PC,[23] Fe_3O_4/PDA,[25]

367    $Fe_3O_4@SiO_2$-G,[26] MIL-101,[27] $Fe_3O_4/SiO_2/TPA$,[28] IL-MNPs[29] and nylon 6 [30] reported

368   in literatures. The sorbent amount, loading volume, LODs, RSDs and recoveries

369   obtained with different materials are listed in Table 3. The proposed sorbent shows

370   similar extraction efficiency to other reported sorbents.[23,26,27,28,30] The LODs of the

371   proposed method were comparable with those methods [16,18,20,23,25,26,28] that

372   HPLC-FLD was also used. Besides the sample volume, less amount of

373    $Fe_3O_4@SiO_2@Nap$ sorbent was needed in cmparion with some other

374   MNPs.[3,14,16,18-20,23,28] But in comparion with these sorbents: Fe_3O_4/C,[17]

375    $Fe_3O_4/SiO_2/SiO_2$-C_{18},[21] Fe_3O_4/PDA,[25] $Fe_3O_4@SiO_2$-G,[26] MIL-101[27] and IL-MNPs[29],

376   more amount of $Fe_3O_4@SiO_2@Nap$ was needed. In addition, the abundant π electrons

377   of naphthyl provide potent π-π stacking interactions with PAHs, contributing to the

378   selectivity to PAHs. The adsorption equilibrium in the process of extraction can be

379   quickly achieved due to the good hydrophilicity of Fe3O4@SiO2@Nap. Shorter

380   extraction time was needed than several MSPE methods.[5,17,18,20,21,27,28,30] Considering

381   these results, the proposed sorbent is a sensitive, efficient, convenient and reliable

382　material for the pre-concentration of trace PAHs.

383

4. Conclusions

385　　Naphthyl functionalized magnetic nanoparticles were successfully synthesized

386　as a novel sorbent for the enrichment of PAHs from river water samples. Due to the

387　condensed cyclic structure and hydrophobic property of naphthyl, the

388　$Fe_3O_4@SiO_2@Nap$ magnetic nanoparticles display satisfying extraction efficiency.

389　Compared to other magnetic materials reported in recent years, $Fe_3O_4@SiO_2@Nap$

390　magnetic nanoparticles have some advantages. In the analysis of seven kinds of

391　PAHs in river water samples, the $Fe_3O_4@SiO_2@Nap$ magnetic sorbents showed

392　reliable analytical performance.

Acknowledgements

397

398

399

400

401 Table 2 Results of determination and recoveries of river water samples by MSPE.

Analytes	Yudai river water samples				Qingshan Lake water samples				Ganjiang water samples			
	Found (ng L^{-1})	Added (ng L^{-1})	Recovery (%)	RSDs (%, n=3)	Found (ng L^{-1})	Added (ng L^{-1})	Recovery (%)	RSD (%, n=3)	Found (ng L^{-1})	Added (ng L^{-1})	Recovery (%)	RSDs (%, n=3)
Flu	N.D.[a]	0.5	95.8	2.3	N.D.	0.5	98.1	3.6	N.D.	0.5	92.6	3.8
		5	104.0	1.8		5	104.4	4.7		5	104.4	2.6
		10	92.7	2.9		10	89.9	3.9		10	93.6	4.5
Ant	0.60±0.05	0.5	104.3	4.9	0.73±0.05	0.5	94.8	4.7	0.77±0.05	0.5	105.8	4.2
		5	101.2	3.0		5	101.4	3.3		5	95.2	3.4
		10	95.0	3.4		10	90.5	5.3		10	92.6	2.7
Fla	1.49±0.05	0.5	101.3	4.5	0.86±0.05	0.5	102.4	3.2	N.D.	0.5	103.6	3.8
		5	106.5	5.2		5	103.4	4.2		5	106.6	2.2
		10	94.7	2.8		10	96.8	2.5		10	95.5	3.2
Pyr	N.D.	0.5	106.7	4.8	N.D.	0.5	106.6	2.5	N.Q.[b]	0.5	103.9	4.4
		5	103.9	3.6		5	104.7	5.3		5	105.6	2.9
		10	93.5	3.9		10	95.6	2.7		10	101.5	3.5
BaA	N.D.	0.5	105.7	5.8	N.D.	0.5	104.6	3.2	N.D.	0.5	104.8	5.0
		5	102.5	2.6		5	106.8	4.4		5	102.7	3.2
		10	93.8	4.9		10	94.0	2.9		10	90.4	5.2
BbF	N.D.	0.5	105.8	5.9	N.D.	0.5	106.3	4.1	N.D.	0.5	105.2	3.5
		5	94.8	3.8		5	102.8	5.2		5	94.4	4.3
		10	96.7	3.2		10	95.6	4.9		10	91.4	2.6
BkF	N.D.	0.5	93.8	4.5	N.D.	0.5	106.7	4.1	N.D.	0.5	95.3	3.6
		5	102.7	3.8		5	95.6	3.3		5	93.5	2.8
		10	96.1	4.0		10	89.6	4.7		10	104.6	4.9

402   N.D. [a]: not detected.

403   N.Q. [b]: found but can't be quantified.

404

405

406

407

408

409

410

411

412

413

414

415

416   Table 3 Comparison of the analytical performance of the proposed MNPs with other magnetic nanomaterials

sorbent	Amount of sorbent (mg)	Extraction time (min)	loading volume （mL）	method	LODs (ng L^{-1})	RSDs (%)	Recoveries (%)	Enrichment factor	Ref.
Fe_3O_4/C	50	Very short time	1000	HPLC-FLD	0.2-0.6	0.8-9.7	76-110	n.r.	16
Fe_3O_4/C	10	30	20	GC-MS	15-335	3.6-9.3	n.r.	35-133	17
C_{10}-C_{18} carboxylates	200	18	350	HPLC-FLD	0.1-0.25	1-7	85-94	n.r.	18
OPA/MMNPs	50	1	10	GC-MS	14.1-70.0×10^3	1.2-11.7	61.9-119.1	n.r.	14
magnetic C_{18}	50	6	20	GC-MS	0.8-36×10^3	2.0-10	35-99	n.r.	19
$Fe_3O_4@C_{18}$	100	30	500	HPLC-FLD	2-5	1-8	72－108	n.r.	20
$Fe_3O_4/SiO_2/SiO_2$-C_{18}	30	20	500	HPLC-FLD	n.r.	n.r.	＞60%	n.r.	21
$Fe_3O_4/MPNP$	200	15	200	UHPLC-DAD	10.83-18.53 nM.	0.3-8.2	75.7-106.4	157-186	3
Fe_3O_4/PC	100	10	500	HPLC-FLD	0.2-0.6	1-8	89-115	n.r.	23
Fe_3O_4/PDA	20	5	500	HPLC-FLD	0.5-0.9	1-9.7	76.4-107	n.r.	25
$Fe_3O_4@SiO_2$-G	15	5	250	HPLC-FLD	0.5-5	2.8-5.6	83.2-108.2	137-173	26
MIL-101	1.6	20	20	HPLC-PDA	2.8–27.2	3.1-8.7	81.3-105	101-180	27
$Fe_3O_4/SiO_2/TPA$	50	15	200	HPLC-FLD	0.04-37.5	＜10	80-108.33	n.r.	28
IL-MNPs	30	8	100	GC-MS	0.04-1.11×10^3	4.0-8.9	75-102	49-158	29
nylon 6	40	30	25	HPLC-PDA	0.05-0.58×10^3	3.8-6.8	80-110	18.1-43.5	30
$Fe_3O_4@SiO_2@Nap$	40	12	150	HPLC-FLD	0.04-0.12	0.6-3.0	89.6-106.8	139-163	This work

417   n.r.: not reported.

References

1 P. Boffetta, N. Jourenkova and P. Gustavsson, *Cancer Causes Control*, 1997, **8**, 444-472.

2 J. N. Bianchin, G. Nardini, J. Merib, A. N. Dias, E. Martendal and E. Carasek, *J. Chromatogr. A*, 2012, **1233**, 22-29.

3 X. Zhang, S. Xie, M. C. Paau, B. Zheng, H. Yuan, D. Xiao and M. M. Choi, *J. Chromatogr. A* , 2012, **1247**, 1-9.

4 R. A. Perez, B. Albero, J. L. Tadeo, M. V. Fraile and C. Sanchez-Brunete, *Anal. Methods*, 2014, **6**, 1941-1950.

5 B. Janoszka, *Food Chem.*, 2011, **126**, 1344-1353.

6 C. F. Poole, *TrAC Trends Anal. Chem.*, 2003, **22**, 362-373.

7 M. Šafaříková and I. Šafařík, *J. Magn. Magn. Mater.*, 1999, **194**, 108-112.

8   Y. Zheng, P. D. Stevens and Y. Gao, *J. Org. Chem.*, 2006, **71**, 537-542.

9 J. Yang, J. Y. Li, J. Q. Qiao, H. Z. Lian and H. Y. Chen, *J. Chromatogr. A*, 2014, **1325**, 8-15.

10 L. J. Xie, R. F. Jiang, F. Zhu, H. Liu and G. F. Ouyang, *Anal. Bioanal. Chem.*, 2014, **406**, 377-399.

11 A. Ríos, M. Zougagh and M. Bouri, *Anal. Methods*, 2013, **5**, 4558-4573.

12 Q. Liu, J. Shi, M. Cheng, G. Li, D. Cao and G. B. Jiang, *Chem. Comm.*, 2012, **48**, 1874-1876.

13 G. Giakisikli and A. N. Anthemidis, *Anal. Chim. Acta*, 2013, **789**, 1-16.

14 J. Ding, Q. Gao, D. Luo, Z. G. Shi and Y. Q. Feng, *J. Chromatogr. A*, 2010, **1217**, 7351-7358.

15 F. Bianchi, V. Chiesi, F. Casoli, P. Luches, L. Nasi, M. Careri and A. Mangia, *J. Chromatogr. A*, 2012, **1231**, 8-15.

16 S. Zhang, H. Niu, Z. Hu, Y. Cai and Y. Shi, *J. Chromatogr. A*, 2010, **1217**, 4757-4764.

17 L. Bai, B. Mei, Q. Z. Guo, Z. G. Shi and Y. Q. Feng, *J. Chromatogr. A*, 2010, **1217**, 7331-7336.

18 A. Ballesteros-Gómez and S. Rubio, *Anal. Chem.*, 2009, **81**, 9012-9020.

19 Y. Liu, H. F. Li and J. M. Lin, *Talanta*, 2009, **77**, 1037-1042.

20 S. X. Zhang, H. Y. Niu, Y. Q. Cai and Y. L. Shi, *Anal. Chim. Acta*, 2010, **665**, 167-175.

447   21   X. L. Zhang, H. Y. Niu, W. H. Li, Y. L. Shi and Y. Q. Cai, *Chem. Commun.*, 2011, **47**,
448   4454-4456.

449   22   F. Yang, Y. Long, R. Shen, C. Chen, D. Pan, Q. Zhang, Q. Cai and S. Yao, *J. Sep. Sci.*, 2011,
450   **34**, 716-723.

451   23   S. Zhang, H. Niu, Y. Zhang, J. Liu, Y. Shi, X. Zhang and Y. Cai, *J. Chromatogr. A*, 2012,
452   **1238**, 38-45.

453   24   Z. Yan, J. Yuan, G. Zhu, Y. Zou, C. Chen, S. Yang and S. Yao, *Anal. Chim. Acta*, 2013, **780**,
454   28-35.

455   25   Y. Wang, S. Wang, H. Niu, Y. Ma, T. Zeng, Y. Cai and Z. Meng, *J. Chromatogr. A*, 2013,
456   **1283**, 20-26.

457   26   W. Wang, R. Ma, Q. Wu, C. Wang and Z. Wang, *J. Chromatogr. A*, 2013, **1293**, 20-27.

458   27   S. H. Huo and X. P. Yan, *Analyst*, 2012, **137**, 3445-3451.

459   28   Y. M. Long, Y. Z. Chen, F. Yang, C. Y. Chen, D. Pan, Q. Y. Cai and S. Z. Yao, *Analyst*, 2012,
460   **137**, 2716-2722.

461   29   F. Galán-Cano, M. D. C. Alcudia-León , R. Lucena, S. Cárdenas and M. Valcárcel, *J.*
462   *Chromatogr. A*, 2013, **1300**, 134-140.

463   30   E. M. Reyes-Gallardo, R. Lucena, S. Cárdenas and M. Valcárcel, *J. Chromatogr. A*, 2014,
464   **1345**, 43-49.

465   31   United   States   Environmental   Protection   Agency   (1984)   Method   610   -PNAs.
466   EPA-600/4-84-063. Environmental Monitoring and Support Laboratory, Cincinati.

467   32   Z. Y. Ma, Y. P. Guan and H. Z. Liu, *J. Polym. Sci. Polym. Chem.*, 2005, **43**, 3433-3439.
468
        33   E. Martinez, M. Gros, S. Lacorte and D. Barceló, *J. Chromatogr. A*, 2004, **1047**, 181-188.

469   34   C. S´anchez-Brunete, E. Miguel and J. L. Tadeo, *J. Chromatogr. A*, 2007, **1148**, 219-227.

470   35   F. Suna, D. Littlejohnb and M. D. Gibson, *J. Chromatogr. A*, 1998, **364**, 1-11.

471

472

473

474

Figure Legends

Fig.1. Preparation scheme of $Fe_3O_4@SiO_2@Nap$

Fig.2. Magnetization curves of Fe_3O_4, $Fe_3O_4@SiO_2$ and $Fe_3O_4@SiO_2@Nap$ (a), FTIR spectroscopy of Fe_3O_4, $Fe_3O_4@SiO_2$ and $Fe_3O_4@SiO_2@Nap$ (b), Detail and deconvoluted XPS spectra of C 1s, N 1s, O 1s and Si 2p for $Fe_3O_4@SiO_2@Nap$ (c)..

Fig.3. Effect of (a) amount of sorbent, (b) different desorption solvent, (c) the sample volume, (d) extraction time on the extraction recoveries of PAHs.

Fig.4 Comparison of different sorbents on the extraction efficiencies of PAHs

Fig.5. Magnetic solid-phase extraction HPLC-FLD chromatograms of river water samples. (a) Qingshan Lake river water sample spiked with 5 ng L^{-1} of each analyte; (b) Ganjiang river water sample; (c) Qingshan Lake river water sample and (d)Yudai river water sample. Peak assignment: (1) Flu, (2) Ant, (3) Fla, (4) Pyr, (5) BaA, (6) BbF, (7) BkF.

498   Table

499   Table 1 Figures and merit of the MSPE method for the determination of PAHs in

500   water.

501   Table 2 Results of determination and recoveries of river water samples by MSPE.

502   Table 3 Comparison of the analytical performance of the proposed MNPs with other

503   magnetic materials

504